

2

3 **Cephalonia-Lefkas Transform Fault Zone**

4 **(CLTFZ) Complexity: Insights from 2015 Lefkas**

5 **earthquake sequence**

6

7

8

---

9

10

11 **ABSTRACT**

12

In order to define a better model for the Cephalonia-Lefkas Transform Fault Zone the sequence of 2015 Lefkas earthquake was examined. On 17 November 2015 (07:10 GMT) a major earthquake ( $M_w=6.4$ ) occurred on the central-western part of Lefkas island. Several destructive events were located in the past in this fault zone, so an extensive seismotectonic study is feasible for that area. Manual analysis was performed using a custom velocity model that was determined for that purpose, applying the average travel-time residuals and location uncertainties errors minimization method. Several clusters belonging to the aftershock sequence were identified, whereas three are directly related to the causative fault, covering an area of about 25 km. The central one, which includes the mainshock, comprises of only a few aftershocks. The northern, within which the majority of aftershocks are located, lies in the central part of Lefkas island and the southern occurred close to the SW edge of the island. In addition, offshore clusters with distinct characteristics have been identified to the south, between Lefkas and Cephalonia islands. The temporal evolution of the aftershock sequence indicates that no migration was observed, given that after the occurrence of the mainshock the entire epicentral area was activated. Focal mechanisms of the Seismological Laboratory of the University of Athens showed dextral strike-slip faulting for both mainshock and major aftershocks of the sequence. Taking into account the spatial distribution of the aftershocks, supported by the tectonic and geomorphological settings of the region, a deformation pattern, consisting of the Cephalonia-Lefkas and Ithaca-Lefkas major fault zones which converge in the area of Vassiliki bay is proposed. The appearance of the southernmost clusters was interpreted by the positive Coulomb stress changes transfer due to major earthquake  $M_w=6.4$ .

13

14 *Keywords: [Seismotectonic analysis; releasing bends; restraining bends; Lefkas aftershock*

15 *sequence; Western Greece]*

16

17

18

19

20

21 **1. INTRODUCTION**

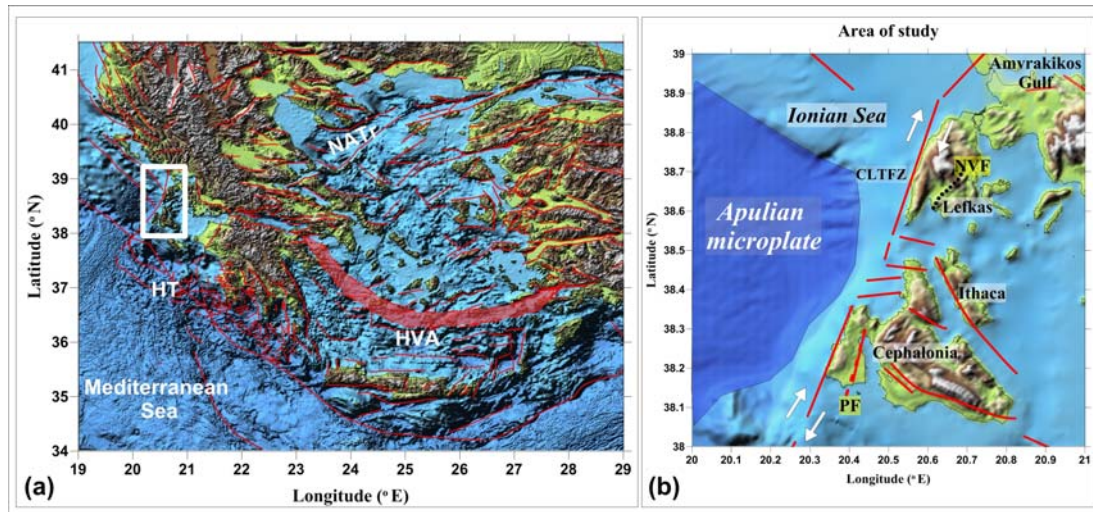
22

23 The Hellenic peninsula is bounded by important geologic and tectonic features such as the

24 Alpine mountain chain to the North, caused by the collision between Europe and Africa [1],

25 the North Anatolian Fault zone to the East, created by the lateral motion of Anatolia with

26 respect to the European tectonic plate [2] and the Hellenic arc to the south, characterized by  
27 the subduction of Tethys oceanic crust [37].



28

29 **Fig. 1. a) Main tectonic and volcanic elements of the broader area of Greece. The**  
30 **study area is highlighted with a white rectangle b) Zoom in the study area of Central**  
31 **Ionian Sea, showing the islands of Cephalonia and Lefkas. Abbreviations in both**  
32 **maps are as following: HT, Hellenic Trench; NATr, North Aegean Trough; HVA,**  
33 **Hellenic Volcanic Arc; CLTFZ, Cephalonia-Lefkas Transform Fault Zone; PF, Paliki**  
34 **Fault; NVF, Nydri-Vassiliki Fault.**

35 The area of Western Greece (Fig. 1.) which is running from the Greek-Albanian borders to  
36 the southern edge of Peloponnese and from the Ionian Islands to eastern Thessaly and  
37 Macedonia lies between a continental collision zone to the north (Adria Microplate-Eurasia)  
38 and the Hellenic Trough to the south, where remnants of the Eastern Mediterranean oceanic  
39 crust subduct under the Aegean continental lithospheric microplate. These zones are linked  
40 with the Cephalonia-Lefkas Transform Fault Zone (CLTFZ), playing an important role in the  
41 geodynamics of the area. Seismological data for the CLTFZ indicate right-lateral strike-slip  
42 focal mechanisms ([31] [28]) which is in agreement with the geodetic data revealing the  
43 NNE-SSW direction of slip motion [11] [21]. The seismic strain rate is well correlated with  
44 the principal horizontal axis of the total geodetic strain rate field. Some smaller neotectonic  
45 structures are mainly expressed by minor faults that strike NNE-SSW to E-W direction,  
46 overprinting the pre-existing thrust-related Plio-Quaternary features, breaking up the island  
47 in multiple independent fault blocks [22].

48 The broader area of study is characterized by a series of NW-SE striking geotectonic units,  
49 such as the Pre-Apulian (or Paxos) and Ionian [9] which form the terrain of External  
50 Hellenides. These structures which have resulted by a subduction-related compressional  
51 regime are coaxial with earlier Alpine structures resulting from the collision of the Pre-  
52 Apulian plate with Eurasia. The mountain chain of Hellenides located between southern  
53 Albania and the Gulf of Corinth plays an important role on the seismotectonics of the region.

54 The Ionian Islands are separated from the mainland by rapidly extensional Pliocene-  
55 Quaternary basins [5] [39] [70]). The oldest sediments that fill those basins are of Pliocene  
56 age. In Lefkas Island, carbonate and clastic sediments belonging to the external geotectonic  
57 units of the Hellenic arc dominate the geological setting [29]. The geotectonic units of Paxos

58 and Ionian are separated by a major west-directed thrust (Aubouin, 1957[3]; [9] which is  
59 marked by Triassic evaporitic intrusions [12].

60 The majority of strong earthquakes in the broader region have mainly occurred along the  
61 main tectonic features, such as the CLTFZ. Lefkas Island is characterized by the occurrence  
62 of large earthquakes, both during the historical and the instrumental era, that have caused  
63 significant damage [25] [32]. Most events were located close to the NW part of the island.  
64 More specifically, the 22 November 1704 (M=6.3), the 12 October 1769 (M=6.7), the 23  
65 March 1783 (M=6.7), the 28 December 1869 (M=6.4) and the 27 November 1914 (M=6.3)  
66 earthquakes were among the most significant. They caused several deaths, injuries,  
67 collapse of buildings, fissures, liquefactions and landslides at the northwestern and central  
68 parts of the island. This is the reason why most epicenters of the historical earthquakes are  
69 located close to the northern end of the CLTFZ, in the Ionian Sea [19] [24]. More recently, on  
70 14 August 2003 (05:14 GMT), a large earthquake (Mw=6.3) with a focal depth of 9 km  
71 occurred close to the NW coast of Lefkas Island [3] [38] [27].

72 On the other hand, only two large events have been located close to the southwestern edge  
73 of the Lefkas Island, an area that belongs to the central part of the CLTFZ. Nevertheless,  
74 important microseismic activity is observed. The two events that are related to this area are  
75 the 22 February 1723 (M=6.7) and the 22 April 1948 (M=6.5) earthquakes. Concerning the  
76 latter event, it caused damage at the SW part of the island, while fissures and tsunami  
77 waves were observed. Two months later, on 30 June 1948, an earthquake of magnitude  
78 M=6.4 occurred at the NW part of the island.

79 A strong earthquake of moment magnitude Mw=6.4 occurred on 17 November 2015 on the  
80 western part of Lefkas Island, causing some damage, landslides and ground fissures. In the  
81 present study, this earthquake sequence is investigated in detail. For that purpose, precise  
82 hypocentral locations are required. The latter were obtained using a local velocity model that  
83 is determined.

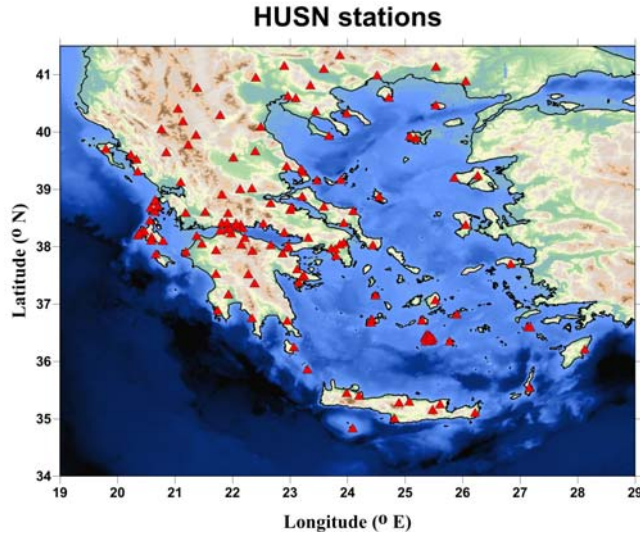
84

## 85 **2. DATA AND METHODS**

86

87 The present study focuses in the area of Central Ionian Islands (Western Greece), where  
88 data of several local stations belonging to the Hellenic Unified Seismological Network  
89 (HUSN) [7] were used for the construction of the local 1D velocity model. HUSN (Fig. 2.)  
90 comprises stations from the Seismological Laboratory of the University of Athens (S.L-  
91 U.O.A), the Geodynamics Institute of the National Observatory of Athens (GE.IN.-N.O.A),  
92 the Geophysical Laboratory of the University of Thessaloniki (G.L.-A.U.TH) and the  
93 Seismological Laboratory of the University of Patras (U.P.S.L.).

94 The data set used in this study comprises of more than 10,000 earthquakes which were  
95 obtained from the seismological stations of HUSN and correspond to the time period 2012-  
96 2017 (Fig. 2). More specifically, all the event locations were calculated using manually  
97 picked P- and S-wave arrival-times, the HYPOINVERSE algorithm [18] a regional 1-D  
98 velocity model, while the duration magnitude was calculated according to the formula  
99 described by relevant studies [16] [28]. A subset of the data catalogue corresponds to the  
100 Paliki (2014) and Lefkas (2015) earthquake sequence, in the vicinity of CLTFZ.



101

102 **Fig. 2. Distribution of HUSN stations (red triangles) throughout Greece**

103

104 **2.1 CONSTRUCTION OF LOCAL VELOCITY MODEL**

105

106 In the present study, the best located events were used to obtain an accurate local 1D  
 107 velocity model for the broader area of Lefkas. The initial locations for the broader area of  
 108 Western Greece were obtained using the regional velocity model derived by [15]. The  
 109 selected events have at least fourteen (14) P- and eight (8) S-wave arrival times. The  
 110 present model was determined by applying the average travel-time residuals and location  
 111 uncertainties errors (RMS, ERX, ERY, ERZ) minimization method [17] [6] [23]. The obtained  
 112 local velocity model (Table 1) yielded improved hypocentral solutions with smaller errors  
 113 than those derived with the initial one (Table 2).

114 **Table 1. Regional and custom velocity model**

Layer	Karakonstantis (2017) $V_p/V_s=1.79$		This Study $V_p/V_s=1.79$	
	$V_p$ (km/s)	Depth (km)	$V_p$ (km/s)	Depth (km)
1	5.3	0.0	4.9	0.0
2	6.0	6.0	5.2	4.0
3	6.3	11.0	5.9	7.0
4	6.5	14.0	6.2	11.5
5	6.7	21.0	6.4	13.0
6	7.3	39.0	6.5	16.0
7	8.0	80.0	7.3	39.0

115

116 The value of  $V_p/V_s$  ratio was obtained using the following methods: a) Chatelain (1978), that  
 117 consists of determining the slope of the straight best-fit line of the difference between  
 118 couples of S-wave and P-wave travel-times for each couple of stations and for each event  
 119 and b) the travel-time residuals and location uncertainties errors (RMS, ERX, ERY, ERZ)  
 120 minimization method. The last mentioned  $V_p/V_s$  ratio determination method follows the  
 121 same procedure that was performed in order to define velocity and ceiling depth for each  
 122 layer. The data for both Chatelain and Spatio-Temporal Error Minimization methods  
 123 converge to the same  $V_p/V_s$  ratio value of 1.79. Error statistics for all spatial groups with

124 both regional and custom local models are presented in Table 2. The mean horizontal (ERH)  
 125 and vertical (ERZ) location errors of the events located in the broader study area are smaller  
 126 than 1 km, while the mean RMS error is 0.132 sec.

127 **Table 2. Statistics of location uncertainties and median depth for the regional**  
 128 **and custom model**

	<b>Karakonstantis (2017)</b>	<b>This Study</b>
Mean RMS (s)	0.139	0.132
Median RMS (s)	0.110	0.110
Mean ERH (km)	1.125	0.909
Median ERH (km)	0.730	0.580
Median ERX (km)	0.510	0.380
Median ERY (km)	1.070	1.050
Mean ERX (km)	0.614	0.459
Mean ERY (km)	1.636	1.360
Mean ERZ (km)	1.933	1.323
Median ERZ (km)	1.310	0.870
Mean Depth (km)	7.542	8.765
Median Depth (km)	6.860	8.375
St.Dev.Y (km)	13.036	13.076
St.Dev.X (km)	6.569	5.963
St.Dev.Z (km)	3.550	3.459

129

130

131

132

## 2.2 COULOMB STRESS TRANSFER

133

134

135

136

In order to investigate the possible acceleration or triggering of the above-observed clusters due to the strong earthquake  $M_w=6.4$ , the Coulomb stress changes transfer was calculated in different depths and cross-sections. The transferred  $\Delta CFF$  was determined on the fault plane with an effective coefficient of friction  $\mu=0.4$  [33] [34].

137

138 **3. RESULTS AND DISCUSSION**

139

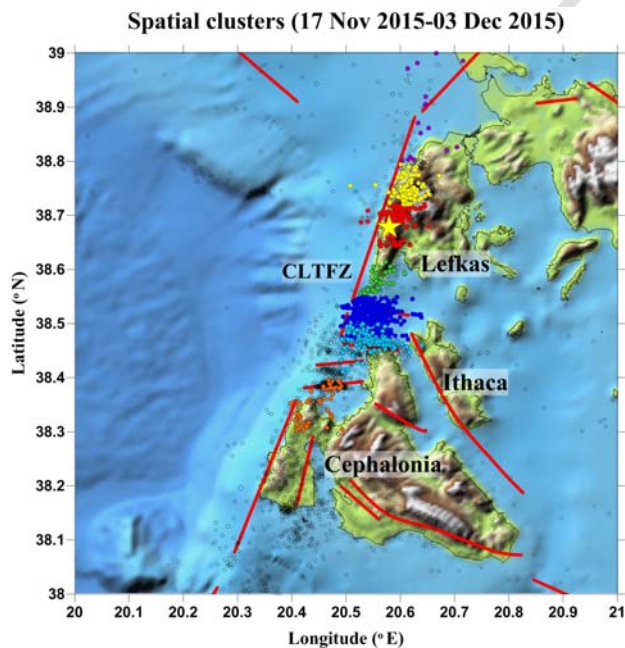
140 On 17 November 2015 (07:10 GMT) a destructive earthquake occurred along the SE coast  
141 of Lefkas Island, in the vicinity of Athani village. There were two fatalities, one due to rockfall  
142 and one caused by a paddock collapse. Eight people were injured, two of which children.  
143 Certain collapses, rockfalls and landslides have been reported.

144 Manual analysis was conducted for the mainshock and for more than 2,500 aftershocks for  
145 the period between 17 November and 3 December 2015, during which the major part of the  
146 ruptured area was activated. Thus, it is considered that this period provides all necessary  
147 information to interpret the 2015 Lefkas seismic sequence.

148 **3.1 Description of clustered seismicity**

149

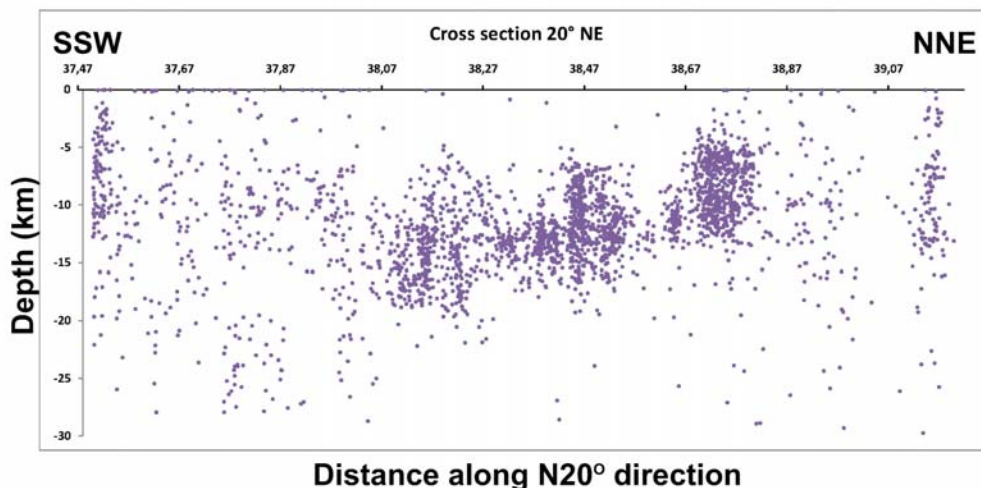
150 The hypocentral locations, using the newly developed 1-D local velocity model, revealed that  
151 the aftershock sequence mainly occurred in the mid-western part of Lefkas Island. However,  
152 another group of events is located S of Lefkas Island, offshore, toward Cephalonia Island. It  
153 is worth noting that the largest aftershock ( $M_w=5.0$ ) occurred near the mainshock on 17  
154 November 08:33 UTC. Both mainshock and the largest aftershock of 17 November 2015 are  
155 well aligned in a SSW-NNE direction. Several linear structures can be distinguished, many of  
156 which offshore, south of Lefkas island, trending roughly E-W. The aftershock distribution  
157 appears mostly aligned in a  $N20^\circ E$  direction with several branches oriented  $\sim N30^\circ E$ ,  
158 including the northernmost and southernmost tips (Fig. 3.).



159

160 **Fig. 3. Map of the study area showing the seven (7) main spatial clusters marked with**  
161 **different colors: cluster #1 (orange), cluster #2 (cyan), cluster #3 (blue), cluster #4**  
162 **(green), cluster #5 (red), cluster #6 (yellow) and cluster #7 (purple). The back ground**  
163 **seismicity, before and after the main body of the aftershock sequence is marked with**  
164 **grey open circles.**

165 The cross-section drawn at N20°E (Fig. 4.), roughly parallel to the CLTFZ, indicates that the  
 166 total length of the activated area is approximately 60 km. The focal depths are distributed  
 167 between 5 and 15 km, with the clusters in the northern group (5 - 7) being generally  
 168 shallower than those of the southern group (1 - 4). The mainshock, as well as the strongest  
 169 aftershock (Mw=5.0) of 17 November are contained in cluster #5.



170

171 **Fig. 4. SSW-NNE cross-section of the main body of the aftershock sequence. Top axis**  
 172 **is marked by the values of latitude (°N) that the thin section passes by.**

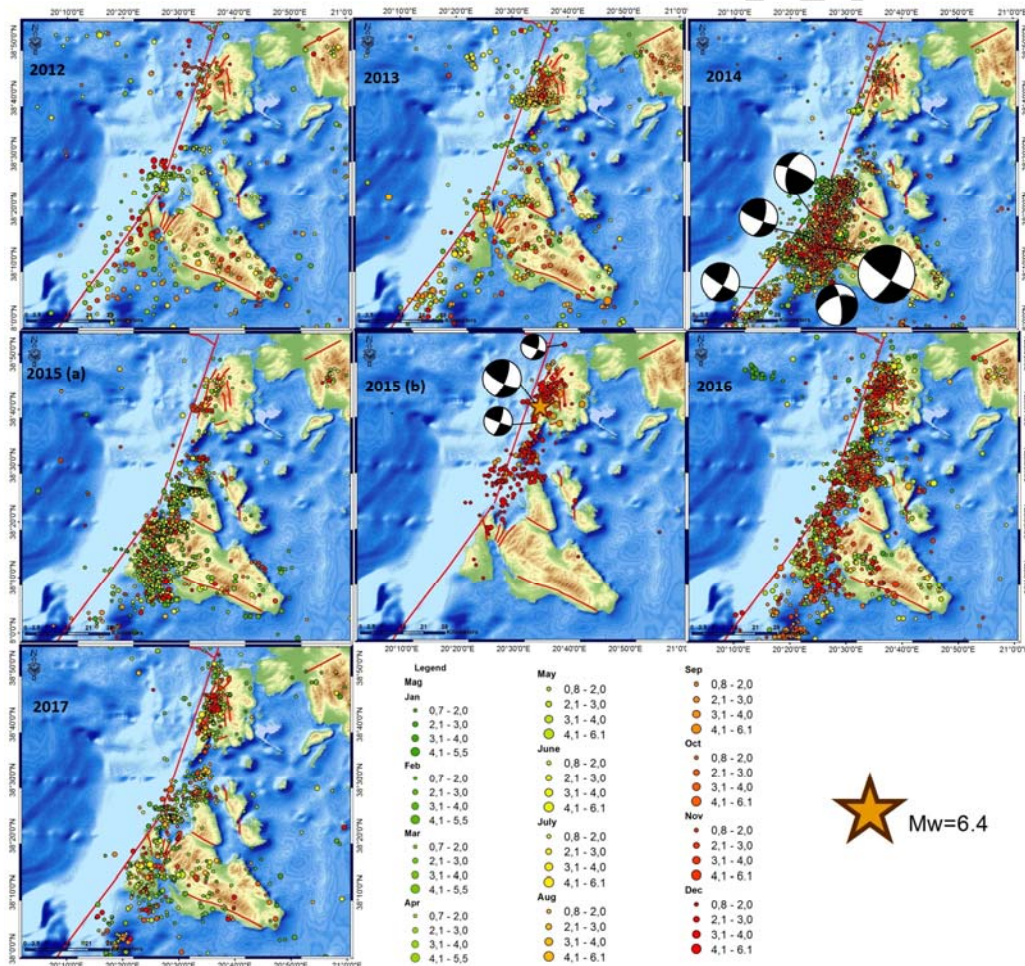
173 The epicenter of the major events of this cluster are mainly aligned SSW-NNE, with the  
 174 smaller sub-cluster being apparently oriented E-W near Vassiliki bay. By far the largest  
 175 cluster is #6, which contains more than 100 events of the aftershock sequence (17/11/2015-  
 176 03/12/2015). Cluster #6 is divided in two branches in its shallower parts (4-6 km), one SSW-  
 177 NNE, similar to cluster #5, and another trending WSW towards the western coast and  
 178 extending a bit deeper (8-9 km) ENE. The described hypocentral distribution is probably  
 179 related to fault network complexity, which has possibly acted as a barrier, prohibiting the  
 180 main rupture to extend further north. It also contains most of the major aftershocks (13  
 181 events with Mw≥3.9) which are, on average, located at slightly larger focal depths (~10 km)  
 182 than the smaller ones (~6 km). Further north, cluster #7 extends ~17 km and deepens from  
 183 ~6 km onshore (excluding a few sparsely located shallower events) down to ~15 km and  
 184 includes the second largest aftershock (Mw=5.0) which occurred on 18 November 2015,  
 185 12:15 UTC. The cluster could be further divided in 2 sub-clusters, the one for the shallower,  
 186 roughly onshore events, trending S-N and the other, offshore further north, containing fewer  
 187 events and apparently trending SW-NE.

188 At the southern group, the northern tip of cluster #4 is ~4-5 km south of the mainshock and  
 189 the cluster extends about 8 km SSW while its median focal depth (~12 km) is larger than the  
 190 one for cluster #5 (~9 km). It probably belongs to the same fault plane as the one of the main  
 191 rupture and defines its deeper seismogenic part. Clusters #2 and #3 are less dispersed than  
 192 cluster #4 and their distribution is roughly oriented E-W. Cluster #2, in particular, contains 2  
 193 large sub-clusters at 8 – 13 km depth and a smaller sub-cluster at 15 km depth. The  
 194 southernmost cluster #1 is a bit offset from the cross-section line (Fig. 4). Its main body is  
 195 located at 7-9 km depth and it also includes several sub-clusters dispersed further south.  
 196 At the very southern edge of the study area, a group of 3 deeper events at ~23-24 km, with  
 197 epicenters between Ithaki and Cephalonia islands, are also included in cluster #1.

198 The Lefkas 2015 aftershock sequence is typical in terms of its spatio-temporal  
 199 characteristics. Aftershocks were generated at both northern and southern edges of the  
 200 zone within minutes to hours following the mainshock, as evident from S.L-U.o.A catalogue  
 201 ([http://www.geophysics.geol.uoa.gr/stations/gmaps3/leaf\\_significant.php?mapmode=mech&ng=en&year=2015#mapanc](http://www.geophysics.geol.uoa.gr/stations/gmaps3/leaf_significant.php?mapmode=mech&ng=en&year=2015#mapanc)) while the largest one ( $M_w=5.0$ ) occurred in less than 2 hours  
 202 after the main event, in the same cluster. By the end of December 2015, the activity in most  
 203 of the spatial groups had diminished (Fig. 5), with the exception of cluster #6, and the  
 204 sequence was typically over, as confirmed by routine observations of the seismicity rate  
 205 during the following months.  
 206

### 207 3.2 Focal Mechanisms

208  
 209  
 210 Fault plane solutions of the largest aftershocks ( $M_w \geq 5.0$ ), determined by the Seismological  
 211 Laboratory of the University of Athens (S.L-U.o.A; [www.geophysics.geol.uoa.gr](http://www.geophysics.geol.uoa.gr)), indicate  
 212 dextral strike-slip faulting. As an example, the focal mechanism of the largest ( $M_w=5.0$ )  
 213 aftershock that occurred on 17 November 2015 (08:33 GMT), 4 km SSW of the mainshock,  
 214 is presented in Fig. 5.

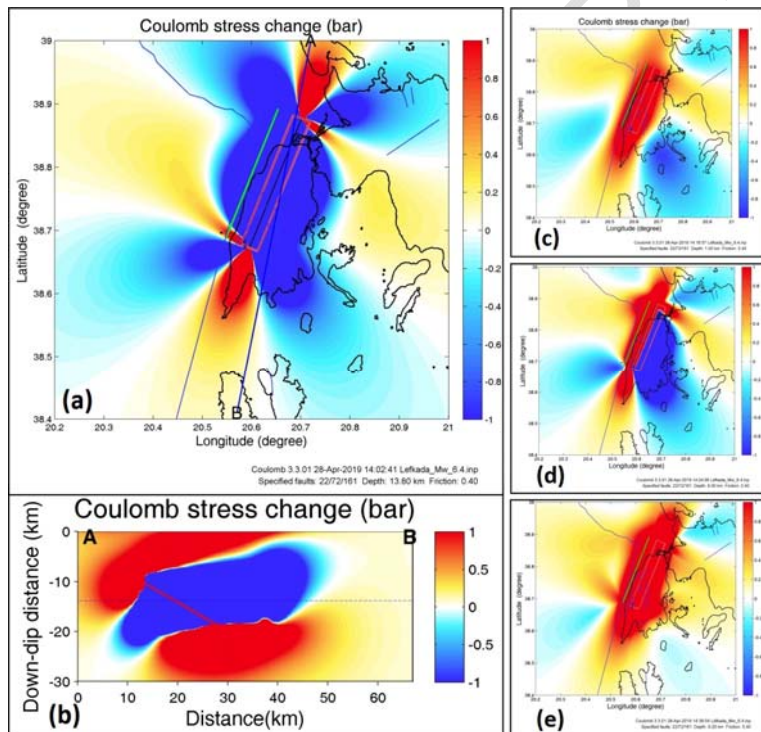


215  
 216 **Fig. 5. Evolution of the seismicity in the study area before (2012-2015a) and after**  
 217 **(2015b-2017) the occurrence of November 17, 2015  $M_w=6.4$  Lefkas earthquake.**

218 Focal mechanisms revealed the activation of an almost vertical right lateral strike slip fault, in  
 219 agreement with the ENE-WSW oriented CLTFZ. The obtained results indicate that the  
 220 dimensions of the activated fault, located between the main aftershock cluster in the central  
 221 part of the island and the one that occurred SSW of Lefkas, are 25 km length and 10 km  
 222 width. The focal mechanisms of the events located offshore, between Lefkas and  
 223 Cephalonia Islands, are similar to the one of the mainshock. Nevertheless, taking into  
 224 account additional characteristics, such as the spatial distribution of the aftershocks and the  
 225 shallower bathymetry, both planes of the focal mechanism of the offshore events could be  
 226 considered as the activated fault, as it will be discussed in more detail in the following  
 227 section.

### 228 3.3 Coulomb Stress Transfer results

229  
 230 The  $\Delta$ CFF distribution is presented, as well as the cross section parallel to the fault in figure  
 231 6a and 6b, respectively. The Coulomb stress distribution showed that the earthquake with  
 232 magnitude  $M_w=6.4$  caused strong positive stress changes transfer in the directions NNW  
 233 and SSE, (Fig. 6c.) as well as in the upper layers from the depth of 8Km until the surface  
 234 (Fig. 6d.). Additionally, the max stress coulomb values were calculated for a depth range 0-  
 235 20Km with step 2Km (Fig. 6e.). The results lead to the conclusion that the southernmost  
 236 clusters are triggered due to the positive Coulomb stress transfer during the fault rupture  
 237 which occurred on the central-western part of Lefkada island, on 17 November 2015,  
 238 ( $M_w=6.4$ ). It is worth noting that the same procedure was observed for the 2003 Lefkas  
 239 rupture process [27].



240  
 241  
 242 **Fig. 6. Distribution maps of Coulomb stress changes ( $\Delta$ CFF) due to the 2015**  
 243 **earthquake  $M_w=6.4$  at the focal depth (a) and cross section AB for strike  $10^\circ N$  (b).**  
 244  **$\Delta$ CFF Maps for depths 1Km (c), 7Km (d), respectively. Max values of Coulomb stress**  
 245 **changes for depth range 0-20Km (e).**

246

247

248

### 3.4 Discussion

249

250

251

252

253

254

255

256

257

258

259

260

261

262

263

264

265

The 2015 Lefkas aftershock sequence is characterised by the existence of several clusters. However, the spatial distribution of the sequence revealed the activation of a large area that extends further than the mainshock's rupture length. Its first characteristic is that only few aftershocks are located in the vicinity of the epicenter. On the contrary the most important cluster is located at the central part of the island. It is characterized by high concentration of epicenters, constituting the main cluster, and is observed towards the northern end of the activated fault segment, at the mid-northern part of Lefkas Island. In the same area, an important cluster occurred during the 1994 sequence, as described by [27]. More specifically, on 29 November 1994 a moderate event of  $M_w=5.1$  took place on the northern part of CLTFZ, close to the west coast of Lefkas Island, followed by a  $M=4.8$  aftershock on 1 December 1994. Aftershock activity was concentrated in the west-central part of the island, in the region where the main cluster of the 2015 sequence occurred. In addition, the 1994 sequence was characterized by an almost vertical distribution, reaching 12 km depth [27]. The above-mentioned observations suggest that this area produces a complex seismicity pattern, which is probably due to the existence of a local minor fault system. This is supported by the high seismicity level that is observed in the central part of Lefkas Island following the occurrence of moderate or large local events.

266

267

268

269

270

271

272

273

274

275

276

277

278

279

280

281

In addition, spatially clustered seismic activity occurred to the south, close to the NNW part of Cephalonia Island, probably not directly related to the main activated fault since they are not located along the CLTFZ but are shifted eastwards forming a step over of the ruptured zone. The southern clusters (#1, #2 and #3) are stretched in a roughly WNW-ESE direction, separated by gaps between them, possibly indicating parallel small left-lateral structures, transverse to the main CLTFZ. Another couple of small clusters of undefined geometry are located near the southern coast of Lefkas (spatial group #4). Other than that, the vicinity of the mainshock's hypocenter is characterized by a few sparse aftershocks. The area defined by the spatial groups #5 and possibly #4 is considered to be the main rupture area, likely a barrier that left a few unbroken asperities where the seismic clusters are observed. However, certain clusters occurred to the south, between Lefkas and Cephalonia Island. Taking them into account, the spatial distribution spans roughly ~60 km in a SSW-NNE direction, while focal depths vary between 5 km (mostly onshore) and 15 km (offshore). The temporal evolution of the aftershock sequence is generally smooth. No significant migration patterns were observed, as almost the full extent of the aftershock zone was activated within the first 24 hours after the mainshock.

282

283

284

285

286

287

288

289

290

291

292

293

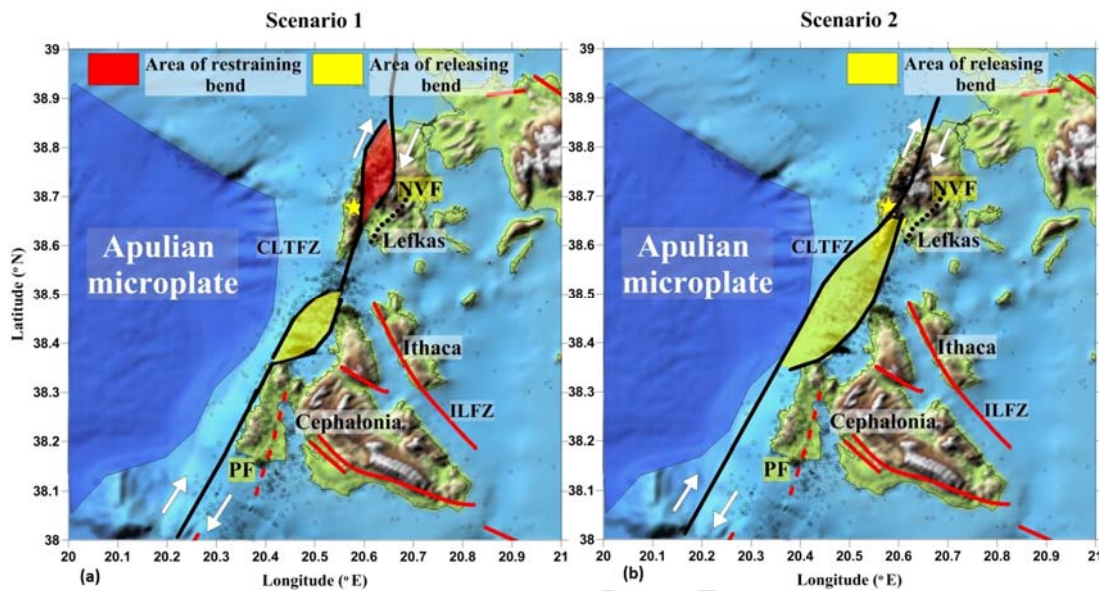
294

295

296

Recent seismotectonic studies suggest that either the CLTFZ in this area is collinear with its northern segment west of Lefkas, while further south it is shifted by some kilometers to the west of Cephalonia coast due to a transfer zone of extensional step overs [8] [13] or that the CLTFZ does not consist of a single dextral strike-slip fault, but rather a system of faults. Even though the 2015 Lefkas aftershock sequence was mainly distributed in the northern segment of the studied fault zone, some significant spatial clusters to the south of Lefkas Island appeared almost perpendicular, in a mean WNW-ESE direction, with the focal mechanisms implying sinistral strike-slip faulting. The results of the present study are in general fairly correlated to the scenario of previous seismological studies in the area [14], with the exception of the smaller than expected, according to their model, fault's dimensions, taking into account the southern clusters of the 2015 Lefkas sequence. Thus, the perpendicular secondary fault system of the latter model has to be prolonged towards the north, up to the southern part of Lefkas. In that case, the negative flower structure model, proposed by [14], could be adjusted by making a double left-bend which explains lots of the superficial geological and geomorphological features at the SW edge of Lefkas (e.g. [22] [26]

297 [2] [35]). The advantage of this model is that it explains the observed seismicity south of  
 298 Lefkas, while its disadvantage is the steep bending of the main part of the fault zone which is  
 299 not compatible with the rupture process of the mainshock (Fig. 7a.).



300

301 **Fig. 7. a) Double left-bend of CLTFZ model (scenario 1) and b) two major converging**  
 302 **fault zones (CLTFZ and ILFZ), forming an almost antithetic system of strike-slip faults**  
 303 **(scenario 2).**

304

305 Another scenario, which fits most of the results obtained by this study, is combined with  
 306 previous knowledge based on GPS measurements (e.g. [30]), geophysical (e.g. [20])  
 307 geomorphological and tectonic elements at the southern part of Lefkas and the sea-bottom  
 308 of Myrtos Gulf (e.g. [22] [2] [35]). It includes two major fault zones, the CLTFZ and Ithaca-  
 309 Lefkas (ILFZ), converging in the area of Vassiliki bay forming en-echelon arrays of WNW-  
 310 ESE minor faults and fractures, separated by smaller NE-SW strike-slip faults in between  
 311 (Fig. 12), such as the one of Nydri-Vassiliki (NVF). In this model, there is the major NNE-  
 312 SSW striking CLTFZ offshore, which makes a right bend NW of Myrtos bay, forming a  
 313 releasing bend in a region SSW of Lefkas Island, as in California's deformation model  
 314 described by [36]. On the other hand, the NNW-SSE ILFZ and CLTFZ converge in western  
 315 Lefkas Island, forming an antithetic system of strike-slip faults to the overall sense of the  
 316 zone's shear, comprising crustal rotated blocks of oblique minor faults in the area between  
 317 Cephalonia and Lefkas Islands (Fig. 7b.).

318

319

320

#### 4. CONCLUSION

321

322 The 17 November 2015 Mw=6.4 Lefkas earthquake is located at the southwestern part of  
 323 the island and can be considered as the continuation of the 2003 ruptured area, which  
 324 probably left an unbroken patch. It is obvious that the recent event occurred within this  
 325 asperity. Taking into account both events, the activated area, with a length of about 45 km in  
 326 a SSW-NNE direction, covers the northern part of CLTFZ that is located west of Lefkas. This  
 327 observation implies that the accumulated energy was released in two separate events  
 328 instead of one, which would obviously have considerably larger magnitude. Such earthquake

329 sequences, consisting of more than one event, have been reported since the historical  
330 times, as in the case of the earthquakes that occurred during 1948 [25].

331 The main characteristic of the sequence is that only a few aftershocks with  $M \geq 3.0$  are  
332 located close to the mainshock's epicentre, suggesting that during the rupture process, no  
333 unbroken patches were left at the central part of the activated fault. The southern part of the  
334 activated fault, reaching the SW edge of Lefkas Island, is characterized by low seismicity.  
335 Concluding, the total length of the causative fault is of the order of 25 km, while the  
336 seismicity belonging to the southern and northernmost (1-3 and 7) clusters is probably not  
337 directly related to the CLTFZ. The length of the total activated area is about 60 km, much  
338 larger than the expected rupture length for a  $M_w=6.4$  mainshock. This observation suggests  
339 that the clusters #1, #2, #3 and #7 have been triggered by stress-transfer.

340 The majority of the determined focal mechanisms are similar, related to dextral strike-slip  
341 faulting that was also revealed for the two earthquakes that occurred in Cephalonia during  
342 January – February 2014 [28]. The events located close to Lefkas Island are related to the  
343 main tectonic feature of the area, which is the Cephalonia-Lefkas Transform Fault Zone,  
344 along which other significant earthquakes occurred in the past, such as the 1983 Cephalonia  
345 earthquake. According to the results of the present study, the ruptured fault, with a length of  
346 approximately 25 km, is the prolongation of the 2003 Lefkas earthquake causative fault.

347 The occurrence of the 2015 Lefkas earthquake sequence provided the opportunity to obtain  
348 a more detailed deformation pattern, especially for the area between Lefkas and Cephalonia  
349 islands. For that purpose, two major scenarios are investigated. The first is a negative flower  
350 structure model prolonged towards the southern part of Lefkas. The other scenario includes  
351 the Cephalonia-Lefkas and the Ithaca-Lefkas major fault zones, converging in the area of  
352 Vassiliki bay, separated by smaller strike-slip faults in between, almost perpendicular to the  
353 CLTFZ. Considering the second scenario, both the WNW-ESE clustered seismicity, between  
354 the islands of Cephalonia and Lefkas, and the uplift region in the SW part of Lefkas Island,  
355 can be reasonably explained.

356

## 357 **COMPETING INTERESTS**

358

359 "Authors have declared that no competing interests exist."

360

361

362

363

364

## 365 **REFERENCES**

366

367 1. Anderson H, Jackson J. Active tectonics of the Adriatic Region. *Geophysical Journal of*  
368 *the Royal Astronomical Society*, 91: 937-983. 1987;doi:[10.1111/j.1365-246X.1987.tb01675.x](https://doi.org/10.1111/j.1365-246X.1987.tb01675.x)

369 2. Bathrellos G, Antoniou V, Skilodimou H. Morphotectonic characteristics of Lefkas Island  
370 during the Quaternary (Ionian Sea, Greece). *Geologica Balcanica*. 2009;38:23-33.

371 3. Benetatos C, Kiratzi A, Roumelioti Z, Stavrakakis G, Drakatos G, Latoussakis I. The 14  
372 August 2003 Lefkas Island (Greece) earthquake: Focal mechanisms of the mainshock and  
373 of the aftershock sequence. *Journal of Seismology*. 2005;9(2):171-190.

374 4. Bornovas J. Géologie de l'île de Lefkade. *Geol. and Geophys. Research (I.G.S.R.)*.  
375 1964;10:142pp.

- 376 5. Brooks M, Ferentinos G. Tectonics and sedimentation in the Gulf of Corinth and the  
377 Zakynthos and Kefallinia channels, western Greece. *Tectonophysics*. 1984;101: 25–54.
- 378 6. Chiarabba C, Frepoli A. Minimum 1D velocity models in Central and Southern Italy: a  
379 contribution to better constrain hypocentral determinations. *Ann. Geophys.* 1997;40(4):937-  
380 954.
- 381 7. D’Alessandro A, Papanastassiou D. Baskoutas I. Hellenic Unified Seismological Network:  
382 an evaluation of its performance through SNES method, *Geophys. J. Int.* 2011;185, 1417–  
383 1430.
- 384 8. Hatzfeld D, Karakostas V, Ziazia M, Selvaggi G, Leborgne S, Berge C, et al. The Kozani-  
385 Grevena (Greece) earthquake of May 13, 1995, a seismological study, *Journal of*  
386 *Geodynamics*. 1998 26 (2–4):245-254.
- 387 9. Jacobshagen VH. *Geologie von Griechenland. Beiträge zur regionalen Geologie der Erde*  
388 19. Berlin. 1986.
- 389 11. Kahle HG, Muller MV, Veis G. Trajectories of crustal deformation of western Greece from  
390 GPS observations 1989–1994. *Geophys. Res. Lett.* 1996;23(6):677–680.
- 391 12. Karakitsios V, Rigakis N. Evolution and petroleum potential of Western Greece. *J. Pet.*  
392 *Geol.* 2007;30:197–218.
- 393 13. Karakostas V, Papadimitriou E. Fault complexity associated with the 14 August 2003  
394 Mw6.2 Lefkas, Greece, aftershock sequence. *Acta Geophys.* 2010;58(5):838–854.
- 395 14. Karakostas V, Papadimitriou E, Mesimeri M, Gkarlaouni C, Paradisopoulou P. The 2014  
396 Kefalonia doublet (Mw6.1 and Mw6.0), central Ionian islands, Greece: seismotectonic  
397 implications along the Kefalonia transform fault zone. *Acta Geotech.* 2014:1–16  
398 <http://dx.doi.org/10.2478/s11600-014-0227-4>.
- 399 15. Karakonstantis A. 3-D simulation of crust and upper mantle structure in the broader  
400 Hellenic area through Seismic Tomography. Dissertation, National and Kapodistrian  
401 University of Athens. 2017. Greek
- 402 16. Kaviris G, Papadimitriou P, Makropoulos K. Magnitude Scales in Central Greece. *Bull.*  
403 *Geol. Soc. Greece.* 2007;XXX(3):1114-1124.
- 404 17. Kissling E, Ellworth WL, Eberhart-Phillips D, Kradolfer U. Initial reference models in local  
405 earthquake tomography, *Journal of Geophysical Research.* 1994;99:19635–19646.
- 406 18. Klein FW. Users guide to HYPOINVERSE-2000: A Fortran program to solve for  
407 earthquake locations and magnitudes. U.S. Geol. Surv. Open-File Rept. 02-171, version 1.0.  
408 2002. Available: <https://pubs.usgs.gov/of/2002/0171/pdf/of02-171.pdf>
- 409 19. Kouskouna V, Makropoulos KC, Tsiknakis K. Contribution of historical information to a  
410 realistic seismicity and hazard assessment of an area. The Ionian Islands earthquakes of  
411 1767 and 1769: historical investigation. In: Stucchi, M. (Ed.), “Historical Investigation of  
412 European Earthquakes,” Materials of the CEC project “Review of Historical Seismicity in  
413 Europe”. 1993;(1):195–206.

- 414 20. Kokinou E, Kamberis E, Vafidis A, Monopolis D, Ananiadis G, Zelilidis A. Deep seismic  
415 reflection data from offshore western Greece: A new crustal model for the Ionian Sea,  
416 *Journal of Petroleum Geology*. 2005;28(2):185-202.
- 417 21. Lagios E, Sakkas V, Papadimitriou P, Damiata BN, Parcharidis I, Chousianitis K, et al.  
418 Crustal deformation in the Central Ionian Islands (Greece): results from DGPS and DInSAR  
419 analyses (1995-2006). *Tectonophysics*. 2007;444:119–145.
- 420 22. Lekkas E, Danamos G, Lozios S. Neotectonic structure of Lefkas Island, *Bull. Geol. Soc.*  
421 *Greece*, XXXIV. 2001;(1):157-163.
- 422 23. Lopes AEV, Assumpção M. Genetic Algorithm Inversion of the Average 1D Crustal  
423 Structure using Local and Regional Earthquakes. *Computers & Geosciences*.  
424 2011;doi:10.1016/j.cageo.2010.11.006.
- 425 24. Makropoulos KC, Kouskouna V. The Ionian Islands earthquakes of 1767 and 1769:  
426 seismological aspects. Contribution of historical information to a realistic seismicity and  
427 hazard assessment of an area. In: Albin, P., Moroni, A. (Eds.). "Historical Investigation of  
428 European Earthquakes," Materials of the CEC Project "Review of Historical Seismicity in  
429 Europe". 1994;2:27–36.
- 430 25. Makropoulos K, Kaviris G, Kouskouna V. An updated and extended earthquake  
431 catalogue for Greece and adjacent areas since 1900, *Nat. Hazards Earth Syst. Sci*.  
432 2012;12:1425-1430.
- 433 26. Margaris B, Papaioannou C, Theodulidis N, Savvaidis A, Anastasiadis A, Klimis N, et al.  
434 "Preliminary Observations on the August 14, 2003 Lefkas Island (Western Greece)  
435 Earthquake", EERI Special Earthquake Report, November, (Joint report by Institute of  
436 Engineering Seismology and Earthquake Engineering, National Technical University of  
437 Athens & University of Athens. 2003:1-12.
- 438 27. Papadimitriou P, Kaviris G, Makropoulos K. The Mw = 6.3 2003 Lefkas Earthquake  
439 (Greece) and induced stress transfer changes, *Tectonophysics*. 2006;423:73–82.
- 440 28. Papadimitriou P, Chousianitis K, Agalos A, Moshou A, Lagios E, Makropoulos K. The  
441 spatially extended 2006 April Zakynthos (Ionian Islands, Greece) seismic sequence and  
442 evidence for stress transfer. *Geophys. Jour. Intern*. 2012;190(2):1025-1040.
- 443 29. Renz C. Die vorneogene stratigraphie der normalsedimentaren Formationen  
444 Griechenlands, *Greece. Inst. Geol. Subsurf. Res. Athenes*. 1955;1-637.
- 445 30. Sakkas V, Lagios E, 2015. Fault modelling of the early-2014 ~M6 Earthquakes in  
446 Cephalonia Island (W. Greece) based on GPS measurements. *Tectonophysics*. 2015: 644–  
447 645, 184–196. <http://dx.doi.org/10.1016/j.tecto.2015.01.010>.
- 448 31. Scordilis EM, Karakaisis GF, Karacostas BG, Panagiotopoulos DG, Comninakis PE,  
449 Papazachos B.C. Evidence for transform faulting in the Ionian Sea: the Cephalonia island  
450 earthquake sequence of 1983. *PAGEOPH*. 1985;123:387–397.
- 451 32. Stucchi M, Rovida A, Gomez Capera AA, Alexandre P, Camelbeeck T, Demircioglu MB,  
452 et al. The SHARE European Earthquake Catalog (SHEEC) 1000–1899. *J. Seismolog*.  
453 2013;17(2):523–544.

- 454 33. Toda S, Stein RS, Richards-Dinger K, Bozkurt S. Forecasting the evolution of seismicity  
455 in southern California: Animations built on earthquake stress transfer. *J. Geophys. Res.*  
456 2005;B05S16, doi:10.1029/2004JB003415.
- 457 34. Toda S, Stein R, Lin J, Sevilgen V. Coulomb 3.2, Graphic-rich deformation & stress-  
458 change software. User Guide. 2010.
- 459 35. Triantaphyllou MV. Calcareous nannofossil biostratigraphy of Langhian deposits in  
460 Lefkas (Ionian Islands). *Bulletin of the Geological Society of Greece. Proceedings of the 12th*  
461 *International Congress, 2010;XLII(2):754-762.*
- 462 36. Twiss RJ, Moores EM. *Structural Geology.* W.H. Freeman and Company, New York;  
463 1992.
- 464 37. van Hinsbergen DJJ, van der Meer DG, Zachariasse WJ, et al. *Int J Earth Sci (Geol*  
465 *Rundsch).* 2006; 95: 463. <https://doi.org/10.1007/s00531-005-0047-5>.
- 466 38. Zahradnik J, Serpetsidaki A, Sokos E, Tselentis GA. Iterative Deconvolution of Regional  
467 Waveforms and a Double-Event Interpretation of the 2003 Lefkas Earthquake, Greece. *Bull.*  
468 *Seism. Soc. Am.* 2005;95(1):159–172.
- 469 39. Zeligidis A, Kontopoulos N, Piper DJW, Avramidis P. Tectonic and sedimentological  
470 evolution of the Pliocene-Quaternary basins of Zakynthos Island, Greece: Case study of the  
471 transition from compressional to extensional tectonics. *Basin Research.* 1998;10:393-408.  
472